doi: 10.4149/gpb_2025017

Impact of tauroursodeoxycholic acid and 4-phenylbutyric acid on mitochondrial functions and morphology of SH-SY5Y cells

Monika Liskova[1], Andrea Evinova[2], Jaroslava Guzikova[1], Lubos Hudak[1], Michal Pokusa[2], Lucia Kotulova[2] and Peter Racay[1]

[1] *Department of Medical Biochemistry, Jessenius Faculty of Medicine in Martin, Comenius University in Bratislava, Martin, Slovakia*
[2] *Biomedical Center Martin, Jessenius Faculty of Medicine in Martin, Comenius University in Bratislava, Martin, Slovakia*

Abstract. The aim of our work was to study impact of tauroursodeoxycholic acid (TUDCA), 4-phenylbutyric acid (PBA) and their combination on mitochondrial functions and morphology. TUDCA, PBA and their combination have a significant impact on mitochondrial respiration. Although both TUDCA and PBA are considered to be chemical chaperones influencing endoplasmic reticulum (ER) stress, they affect mitochondrial respiration in a specific way. While TUDCA decreases ROUTINE, maximal, succinate-driven maximal, ATP-coupled and leak respirations; PBA increases spare respiratory capacity (SRC). Combination of TUDCA with PBA increases ROUTINE, maximal, succinate driven maximal and ATP-coupled respirations and SRC. TUDCA, PBA and their combination exhibits positive impact on mitochondria elongation and do not induce expression of proteins involved in mitochondrial fusion and unfolded protein response. Our results do not indicate the impact of either TUDCA or PBA on ER stress since pre-treatment of the cells with either TUDCA or PBA does not significantly affect tunicamycin-induced expression of HRD1, GRP78 and SEL1L. The impact of PBA and combination of TUDCA with PBA on mitochondrial functions might be associated with their possible neuroprotective effects. Although TUDCA exhibits positive effect on inner mitochondrial membrane, the possible neuroprotective effect of TUDCA might involve mechanism distinct from modification of mitochondrial functions.

Key words: Tauroursodeoxycholic acid — 4-phenylbutyric acid — Mitochondria — Endoplasmic reticulum — Neuroprotection

Abbreviations: ER, endoplasmic reticulum; HRR, high-resolution respirometry; PBA, 4-phenylbutyric acid; SRC, spare respiratory capacity; S1PR2, sphingosine-1-phosphate receptor-2; TUDCA, tauroursodeoxycholic acid.

Introduction

Tauroursodeoxycholic acid (TUDCA) is a hydrophilic bile acid naturally produced by conjugation of ursodeoxycholic acid, a secondary bile acid produced exclusively by gut microbiota, with taurine in the liver. TUDCA has been extensively studied for its beneficial effects on liver, metabolic and neurodegenerative diseases. TUDCA and other bile acids are important for liver homeostasis, functioning as signalling molecules that bind to the nuclear receptors, most commonly to the farnesoid X receptor (Jurica et al. 2016). With respect to the diseases distinct from liver, results derived from experiments using cellular and animal models of these

Correspondence to: Peter Racay, Department of Medical Biochemistry, Jessenius Faculty of Medicine, Comenius University, Mala Hora 4D, 03601 Martin, Slovakia
E-mail: peter.racay@uniba.sk

diseases (Khalaf et al. 2022; Xing et al. 2023) showed that protective effects of TUDCA might depend on the binding of TUDCA to the plasma membrane receptors, such as Takeda G protein receptor 5 (TGR5), sphingosine-1-phosphate receptor-2 (S1PR2) and α5β1 integrin (Zangerolamo et al. 2021). The binding of TUDCA to these receptors results in receptor activation, with consequent modulation of complex intracellular signalling network including either activation or inhibition of several different molecular pathways. With respect to the cytoprotective impact of TUDCA, the specific pathways that are modulated by TUDCA are not well understood. However, both ERK and AKT pathways are of specific interest since they are involved in several cytoprotective intracellular responses with an impact on apoptosis, stress of endoplasmic reticulum (ER), oxidative stress, neuroinflammation, cell proliferation and survival. In addition to the plasma membrane receptors, it has been documented that neuroprotective effects of TUDCA depends on binding of TUDCA to the nuclear receptors in neurons (Xing et al. 2023; Duarte-Silva et al. 2024). The mechanisms of TUDCA transport into neuronal cells are still poorly understood. TUDCA can be transported into cells by the Na^+-taurocholate cotransporting polypeptide, however, these channels were only found in hepatocytes (Anwer and Stieger 2014). Some studies have indicated that TUDCA exerts its effects acting as a chemical chaperone that either maintains the stability and correct folding of proteins or prevents aggregation of aberrant proteins (Kusaczuk 2019). The activity of TUDCA as a chemical chaperone was attributed to its putative impact to modulate ER stress (Almanza et al. 2019; Jeon et al. 2022). Mitochondria were also considered to be involved in neuroprotective mechanism mediated by TUDCA in cellular models of Parkinson's disease using SH-SY5Y cells or primary murine cortical neurons (Fonseca et al. 2017; Rosa et al. 2017). TUDCA was approved by the Food and Drug Administration (FDA) for the treatment of biliary cirrhosis. In addition, TUDCA was tested in the several clinical trials as a treatment of neurodegenerative diseases (Khalaf et al. 2022) with a focus on amyotrophic lateral sclerosis (ALS) (Albanese et al. 2022; Lombardo et al. 2023).

Short-chain fatty acid, 4-phenylbutyric acid (PBA), is a derivative of butyric acid that is produced by fermentation of colonic bacteria. Similarly as other short chain fatty acids, inhibition of histone deacetylases (HDAC) represents the main mechanism associated with PBA (Kusaczuk et al. 2015). Inhibition of HDAC triggers specific transcription responses that result in activation/inhibition of different cell signalling pathways. HDAC inhibitors are intensively studied with respect to the treatment of the malignant diseases (Cappellacci et al. 2020). As well as TUDCA, PBA is also considered to act as chemical chaperone leading to the research into its use in diseases associated with protein misfolding such as cystic fibrosis or neurodegenerative diseases (Kolb et al. 2015). The main mechanism associated with protein misfolding cytoprotective action of PBA was attributed to the ability of PBA to alleviate ER stress (Kolb et al. 2015). Finally, PBA exhibits some impact on regulation of lipid metabolism (He and Moreau 2019). PBA was approved by FDA for the treatment of urea cycle disorders. The mechanism involves conjugation of phenylacetyl-coenzyme A that is produced from PBA by β-oxidation with glutamine in the liver (Wright et al. 2011). The conjugation product, phenylacetylglutamine, is released into the blood and, consequently, excreted by the kidney.

Both TUDCA and PBA are blood-brain barrier penetrating substances. Although the precise mode of action remains elusive (Alqallaf et al. 2024), combination of TUDCA and PBA known as AMX0035 was evaluated in ALS in randomized double-blind placebo-controlled Phase III trial (NCT05021536). Despite some promising results of Phase II trial (Paganoni et al. 2023; Sun et al. 2023), AMX0035 is no longer considered for the treatment of ALS (Ketabforoush et al. 2024) but it is further evaluated in Wolfram syndrome (NCT05676034) and progressive supranuclear palsy (NCT06122662).

In this study, we have investigated the effect of both TUDCA and PBA on mitochondrial functions in more details. We have focused our interest on mitochondrial respiration examined by high-resolution respirometry, ATP synthesis capacity evaluated by luciferase-based determination of intracellular ATP concentration, as well as mitochondrial morphology investigated by confocal microscopy in human neuroblastoma cells SH-SY5Y that are often used in neurobiology as an *in vitro* model for the study of neurodegeneration of dopaminergic neurons. Finally, we have performed the Western blot analysis with a focus on selected mitochondrial proteins and key proteins involved in response to stress of ER.

Material and Methods

DPBS (Sigma), trypsine (EC 3.4.21.4, Sigma), ADP (Merck Millipore, 117105), antimycine A (Sigma, A8674), carbonyl cyanide 3-chlorophenylhydrazone (Sigma, C2759), cytochrome c (Sigma, C3131), digitonin (Wako Chemicals, 043-21371), EGTA (Sigma, 03779), HCl (Sigma, 339253), Hepes (Sigma, 54457), KCl (Merck Millipore, 104938), K_2HPO_4 (Sigma, 17835), KOH (Sigma, P5958), MiR05-Kit (Oroboros AT), mannitol (Sigma, M9546), $MgCl_2$ (Sigma, M1028), NaCl (Sigma, 9888), sodium pyruvate (Sigma, P2256), oligomycin (Sigma, O4876), rotenone (Sigma, R885), succinate (Sigma,14080), TUDCA (Merck Millipore, 580549), PBA (Sigma, P21005), tunicamycin (Calbiochem, 504570), mouse monoclonal antibodies against HSP60 (SC-271215, Santa Cruz Biotechnology) and β-actin (3700, Cell Signaling); rabbit polyclonal antibody against MFN1 (sc-50330, Santa Cruz), MFN2 (sc-50331, Santa Cruz),

HRD1 (13473-1-AP, Proteintech), GRP78 (ab227865, Abcam), SEL1L (PA5-88333, Invitrogen), LONP1 (PA5-51692, Invitrogen); goat anti-rabbit (A0545, Sigma-Aldrich) and goat anti-mouse (A0168, Sigma-Aldrich) secondary antibodies conjugated with horse radish peroxidase.

Culturing, treating and harvesting of SH-SY5Y cells

Undifferentiated human neuroblastoma SH-SY5Y cells (ATCC) were cultured at 37°C, 5% CO_2 humidified atmosphere maintained in medium DMEM:F12 (1:1) (Dulbecco's Modified Eagle's Medium and Ham's F-12 Nutrient Mixture, Sigma) supplemented with 10% FBS and 1% penicillin streptomycin stock (all PAA). The medium was changed every 2–3 days until 80% confluence was achieved. SH-SY5Y cells were treated with the indicated concentration of TUDCA, PBA and combination of TUDCA with PBA for 16 h at 37°C and under a 5% CO_2 humidified atmosphere. With respect to ER stress induction, cells were first pre-treated with either TUDCA or PBA for 16 h and then they were further treated with tunicamycin at a concentration of 2 μM in the presence of either TUDCA or PBA for 24 h. At the end of the treatment, the cells were washed 3 times with ice-cold phosphate-buffered saline (PBS) and then resuspended in a lysis buffer (30 mM Tris-HCl, 150 mM NaCl, 1% CHAPS, 1× protease inhibitor cocktail, pH = 7.6) for total protein extraction. Protein concentrations were determined using a protein DC assay kit (Bio-Rad) with BSA as a standard. On the day of high-resolution respirometry analysis, control and treated cells were trypsinised and washed twice with DPBS. An aliquot of cells was lysed and the amount of proteins was determined as described above.

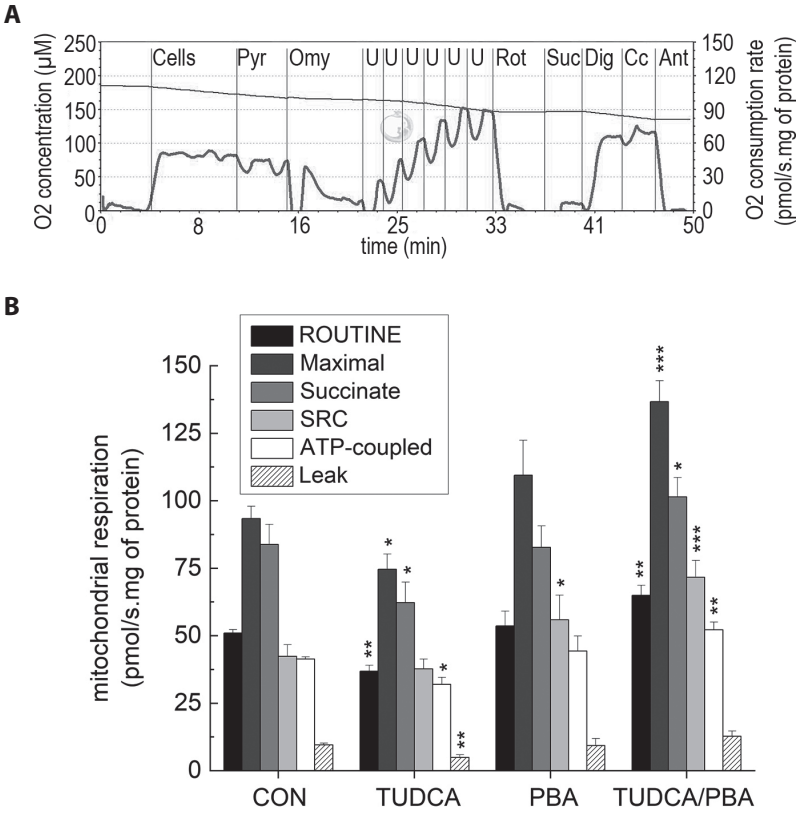

Figure 1. Impact of TUDCA, PBA and combination of TUDCA with PBA on mitochondrial respiration. **A.** Representative record of mitochondrial respiration of SH-SY5Y intact cells. Respiration (oxygen consumption rate) was determined in MiR05-kit respiration medium (Oroboros, Innsbruck AT) at 37°C with continuous stirring (speed 750 rpm) as described in Material and Methods. The vertical lines indicate addition of intact cells, pyruvate (Pyr), oligomycin (Omy), uncoupler CCCP (U), rotenone (Rot), succinate (Suc), digitonin (Dig), cytochrome c (Cc) and Antimycin A (Ant). **B.** Statistical evaluation of mitochondrial respiration. SH-SY5Y cells were treated with TUDCA at a concentration 100 μM, PBA at a concentration 1 mM and combination of 100 μM TUDCA with 1 mM PBA for 16 h. Mitochondrial respiration was assessed using HRR as described in Material and Methods. Data are presented as mean ± S.D. (4 independent experiments *per* each treatment). * $p < 0.05$, ** $p < 0.01$, *** $p < 0.001$ (two-way ANOVA, followed by Tukey's test to determine differences in mitochondrial respiration of treated cells compared to control non-treated cells). CON, control, untreated cells.

High-resolution respirometry (HRR)

Mitochondrial respiration was analysed using HRR measurements of intact cells using the O2k-FluoRespirometer two chamber system (Oroboros Instruments) and the Oroboros coupling control protocol for intact cells as previously described in details (Evinova et al. 2020, 2022).

For the HRR measurements, SH-SY5Y cells (approx. 2×10^6 cells/chamber) were resuspended in respiration medium MiR05-Kit and titrated into 2 ml glass chambers, coupling control protocol for intact cells with the presence of oligomycin was used (Fig. 1A). In accordance with the Oroboros protocols (Pesta and Gnaiger 2012), the resulting O_2 flux values were utilized to calculate respiration in different coupling control states. Residual oxygen consumption (ROX) was evaluated for the flow correction of intact cells respiration. ROUTINE or basal respiration was measured after the addition of the cells into the chambers containing mitochondrial respiration medium. Pyruvate (final concentration 10 mM) as a substrate for intact cells and oligomycin (final concentration 2.5 μM) was used to induce a LEAK state of respiration. ATP-coupled respiration was calculated by subtracting of the value of LEAK state respiration from the value of ROUTINE/basal respiration. Stepwise titration with uncoupler carbonyl cyanide 3-chlorophenylhydrazone (CCCP) (0.5 nmol *per* addition) was used to determine maximal respiration representing the maximal electron transfer capacity of the respiratory system, which is obtained at optimum uncoupler concentration. Spare respiratory capacity (SRC) was calculated by subtracting of the value of ROUTINE respiration from the value of maximal respiration. Rotenone (final concentration 0.5 mM) as an inhibitor of Complex I was used for the determination of ROX. Succinate (final concentration 10 mM) stimulation of mitochondrial respiration was observed only in permeabilized cells after addition of digitonin (stepwise addition 8 μg *per* million cells), providing a reference state of succinate-dependent maximal respiration representing succinate-dependent electron transfer capacity. Cytochrome c titration (final concentration 10 μM) was used to test outer mitochondrial membrane integrity. Antimycin A (final concentration 2.5 mM) as an inhibitor of Complex III was consecutively added at the end of measurement to asses ROX. Values of HRR measurements were normalised to protein concentrations of the lysates of the cells used for HRR measurements.

Determination of intracellular ATP

The ATP Determination Kit (A22066, Thermo Fisher Scientific) was used for the detection of intracellular ATP in cell lysates. SH-SY5Y cells were seeded in 96-well plates at concentrations of 0.1×10^6 cells *per* ml. Control cells and the cells treated with TUDCA and PBA were incubated for 16 h at 37°C under a 5% CO_2 humidified atmosphere. Furthermore, cells were incubated with sodium azide at a concentration of 50 mM for 15 min at 37°C under a 5% CO_2 humidified atmosphere. At the end of the treatment, cultivation medium was carefully aspirated and 0.04 ml of lysis buffer was added (1% CHAPS in 0.04 M Tris-HCl, pH 7.4). Cells were lysed by standing on ice for 30 min. In addition to cell lysates, 0.04 ml of ATP standard solutions with three different concentrations (1.25, 2.5 and 5 μM) diluted in lysis buffer were added to the empty wells. After the addition of 0.3 ml of Standard Reaction Solution (prepared according to the manufacturer's instructions prior to the determination) the chemiluminescence of samples was determined by Synergy H4 Microplate Reader (BioTek). Standard curve for series of ATP concentrations was generated by linear regression using least squares method and the amount of ATP in the experimental samples was calculated from the standard curve. Values of ATP concentrations were normalised to protein concentrations of the lysates that were determined by a protein DC assay kit (Bio-Rad) with BSA as a standard. Results collected from three independent experiments performed in triplicate for each sample are expressed as ATP concentration in cells after particular treatment relative to ATP concentration in control non-treated cells. Data are presented as mean ± standard error of mean (S.E.M.).

Western blotting

Isolated proteins (30 μg proteins loaded *per* lane) were separated on 10% SDS-polyacrylamide gels (PAGE) under reducing conditions. Separated proteins were transferred to nitrocellulose membranes by using semi-dry transfer, and membranes were probed with antibodies specific to HRD1 (1:1000), GRP78 (1:1000), SEL1L (1:1000), MFN1 (1:1000), MFN2 (1:1000), HSP60 (1:1000), LONP1 (1:1000) and β-actin (1:2000). Further incubation of the membranes with particular secondary antibodies (1:10 000 mouse, 1:20 000 rabbit) was followed by the visualisation of immunopositive bands by using the chemiluminiscent substrate SuperSignal West Pico (Thermo Scientific) and the Chemidoc XRS system (Bio-Rad). Intensities of specific bands were quantified by Quantity One software (Bio-Rad). The intensities of the bands of interest were normalised to corresponding intensities of bands of β-actin and were expressed as the intensity of the band of the particular protein in treated cells relative to the intensity of the band in control non-treated cells.

Confocal microscopy and mitochondrial network analysis

Mitochondrial morphology was evaluated using a Zeiss LSM 880 scanning confocal microscope (LSM AxioExaminer platform) with a W Plan-Apochromat 40×/1.0 DIC M27 water-immersion objective. The Mitotracker Red

FM staining (final concentration 500 nM, Thermo Fisher) was performed according to the manufacturer's protocol, incorporating two biological replicates for each experimental group. 64 cells were analysed in total (15 controls, 16 TUDCA, 17 PBA and 16 TUDCA/PBA) for each mitochondrial network parameter under identical acquisition parameters from each biological replicate using a wet objective with 40× magnification. Confocal images were acquired at a resolution of 1024×1024 pixels, with a scaling factor of 0.07×0.07 µm *per* pixel, resulting in a field of view of ~ 71.68×71.68 µm. The scanner zoom was set to X:3.0, Y:3.0, with a pixel dwell time of 8.24 µs. Fluorescence excitation was performed at 561 nm, and emission was detected at 629 nm, ensuring optimal signal capture for Mitotracker Red FM-labeled mitochondria.

For qualitative assessment of mitochondrial morphology changes, the analysis was carried out following a sequence of image processing steps based on the transformation of fluorescence images into binary 2D images. The software protocol was outlined by Bakare et al. (2021), utilizing ImageJ software (FIJI). Parametrisation of the mitochondrial network was performed to facilitate the identification of junctions, branching, length pattern and solitary rod-like mitochondria. The branching pattern was characterised by the proportion of junctions counted against the total number of branches observed in the cell. The average length of the mitochondrial branches was determined by the pixel overlap of separate mitochondrial branch under the same magnification and zoom conditions. The total mitochondrial length in individual cells was calculated by summing length of each mitochondrial branch under the same magnification and zoom conditions. With respect to the characterisation of the fragmentation status, the ratio between the counts of solitary rod-like mitochondria and the overall branches of mitochondria was calculated from the imaged cells.

Statistical analysis

Two-way ANOVA (GraphPad Prism V8.0.2, GraphPad Software) was first carried out to test for differences among all experimental groups (data obtained by HRR, Western blot and ATP level analysis). In addition, the Tukey's test was used to determine the differences between individual groups. Data are presented as either mean ± S.D. or mean ± S.E.M. A $p < 0.05$ was considered significant.

The R programming language (version 4.4.1) (R Core Team, 2024) was used for the analysis of mitochondrial network data. Continuous variables were summarised using the median along with the lower and upper quartiles. Normality and data distribution were assessed through exploratory data analysis, including histograms, Q-Q plots, and boxplots. The symbox and powerTransform functions from the car package (Fox et al. 2023) were utilised to identify the most suitable transformations. Linear models were constructed, each with one of the following response variables: average length of mitochondria, overall mitochondrial length, branching and junction patterns as well as number of solitary rod-like mitochondria. For each model, estimated marginal means (emmeans) were calculated using the emmeans package (Fox et al. 2023) to assess the effect of each group, a four-level predictor. Pairwise comparisons, with Tukey adjustment of *p*-values, were performed to further evaluate differences between group levels.

Results

We have first analysed the impact of both TUDCA and PBA, as well as combination of TUDCA with PBA on mitochondrial respiration after incubation of cells with either TUDCA at a concentration 100 µM or PBA at a concentration 1 mM, as well as with combination of TUDCA at a concentration 100 µM with PBA at a concentration 1 mM for 16 h. The time interval was selected on the basis of previously published data as well as on the basis of our experiments with STF-083010 that indicated its significant impact on mitochondrial respiration after incubation of the cells with STF-083010 for 16 h (Hatokova et al. 2023). The concentrations of both TUDCA and PBA were selected on the basis of previously published results.

Treatment of the cells with TUDCA for 16 h was associated with a significant decrease of ROUTINE respiration (72.4% of control, $p < 0.01$), maximal respiration (79.9% of control, $p < 0.05$), succinate driven maximal respiration (74.3% of control, $p < 0.05$), ATP-coupled respiration (77.3% of control, $p < 0.05$) and LEAK respiration (50,6% of con-

Table 1. Impact of TUDCA, PBA and TUDCA/PBA on intracellular level of ATP

	Relative ATP concentration (% of control)	*p*
Control	100 ± 4	>0.05
TUDCA	111.5 ± 3.2	>0.05
PBA	113.7 ± 5	>0.05
TUDCA/PBA	126.3 ± 10	>0.05
Sodium azide	43.2 ± 1	<0.01

Cells were treated with TUDCA, PBA, TUDCA/PBA and sodium azide and then the concentration of ATP was determined as described in Material and Methods. Data are presented as mean ± S.E.M. (3 independent experiments performed in triplicate *per* each treatment). *p* value was estimated by two-way ANOVA, followed by Tukey's test to determine differences of relative ATP concentration in treated cells in comparison to control non-treated cells.

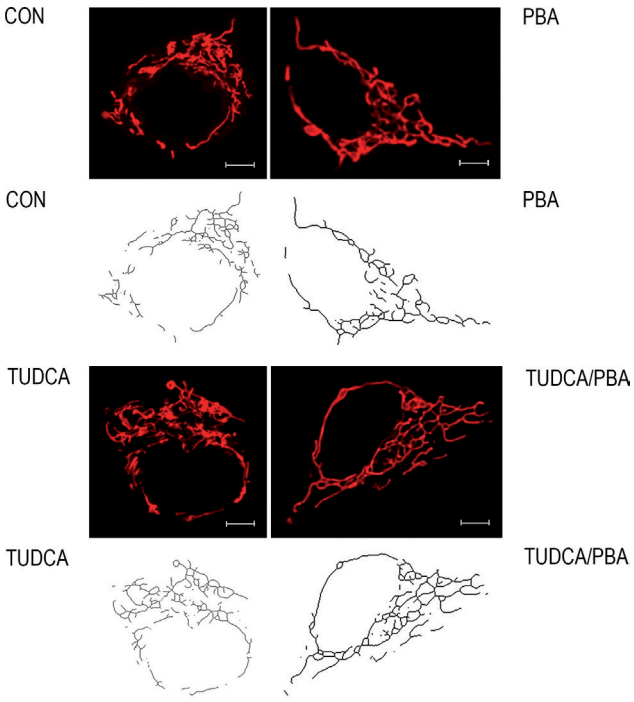

Figure 2. Impact of TUDCA and PBA as well as combination of TUDCA with PBA on the mitochondrial network. Representative images of the cells stained with Mitotracker (scale bar – 5 μm) and schematic illustrations of transformation of obtained images of cellular mitochondrial network to binary images.

trol, $p < 0.01$) (Fig. 1B). The value of SRC capacity was not significantly altered.

Treatment of cells with PBA for 16 h was associated with a significant increase of SRC (131.8% of control, $p < 0.05$, Fig. 1B). The other investigated parameters of mitochondrial respiration were not significantly altered.

Treatment of the cells with combination TUDCA/PBA for 16 h was associated with significant increase of ROUTINE respiration (127.5% of control, $p < 0.01$), maximal respiration (146.4% of control, $p < 0.001$), succinate driven maximal respiration (121% of control, $p < 0.05$), ATP-coupled respiration (126.1% of control, $p < 0.01$) and SRC (169.1% of control, $p < 0.001$) (Fig. 1). LEAK respiration was not significantly altered.

We have further analysed impact of either TUDCA or PBA as well as combination of TUDCA with PBA on intracellular ATP level. Treatment of SH-SY5Y cells with TUDCA and PBA or with combination TUDCA/PBA for 16 h was not associated with significant changes in intracellular ATP levels (Table 1). Treatment of SH-SY5Y cells with sodium azide at a concentration of 50 mM for 15 min that is associated with death of SH-SY5Y cells after 24 h (Klacanova et al. 2016) was associated with significantly decreased ATP level (42.3% of control, $p < 0.01$) (Table 1).

We have also analysed impact of either TUDCA or PBA as well as combination of TUDCA with PBA on mitochondrial network (Fig. 2). Data distribution of mitochondrial network parameters at the experimental group levels are visualised at Figure 3A. *Post-hoc* model analysis (pairwise comparisons of estimated marginal means) of mitochondrial network parameters (Fig. 3B) revealed significantly higher values of overall mitochondrial length in the cells treated with TUDCA ($p < 0.001$), PBA ($p < 0.001$) and combination of TUDCA with PBA ($p < 0.001$). Significantly higher values of branching patterns were determined in the cells treated with PBA ($p < 0.01$) and with combination of TUDCA with PBA ($p < 0.01$). In addition, junction patterns were significantly higher in the cells treated with TUDCA ($p < 0.01$), PBA ($p < 0.01$) and combination of TUDCA with PBA ($p < 0.01$). Average mitochondrial length did not significantly change in all treated cells (data not shown). Furthermore, the fragmentation pattern of the mitochondrial network in cells treated with PBA ($p < 0.01$) and with combination of TUDCA with PBA ($p < 0.01$) was less pronounced, evidenced by significantly reduced count of solitary rod-like mitochondria compared to control non-treated cells.

In order to examine if TUDCA or PBA has an impact on mitochondrial unfolded protein response (UPR) and the intracellular amounts of mitochondria we have performed Western blot analysis of expression of HSP60 and LONP1. Both proteins are considered as important molecular components of mitochondrial UPR (Fiorese et al. 2016). In addition, HSP60 can be considered as a marker of the intracellular content of mitochondria. We have also analysed levels of MFN1 and MFN2 since both proteins are involved in the control of mitochondrial fusion (Giacomello et al. 2020). However, our Western blot analysis did not reveal a significant impact of TUDCA and PBA, as well as combination of TUDCA with PBA, on the expression of investigated proteins (Fig. 4). We have not detected DRP1 phosphorylation (data not shown) at either Ser616 that promotes the translocation of DRP1 from the cytosol to the mitochondrial outer membrane and mitochondrial fission or at Ser637 that reverses this process (Chen et al. 2023).

Since the cytoprotective impact of TUDCA and PBA is often explained by the ability of both substances to modulate ER stress response (Almanza et al. 2019), we have performed a Western blot analysis of the protein extracts prepared from control untreated cells and cells pre-treated with either TUDCA or PBA for 16 h that was followed by the induction of ER stress by the further treatment of the cells for 24 h with tunicamycin at a concentration of 2 μM. The concentration of tunicamycin and the time interval were chosen on the basis of our previous study (Dibdiakova et al. 2019; Evinova et al. 2022). We have focused our interest on the key proteins involved in response to stress of ER. GRP78 is a master protein involved in activation of UPR that

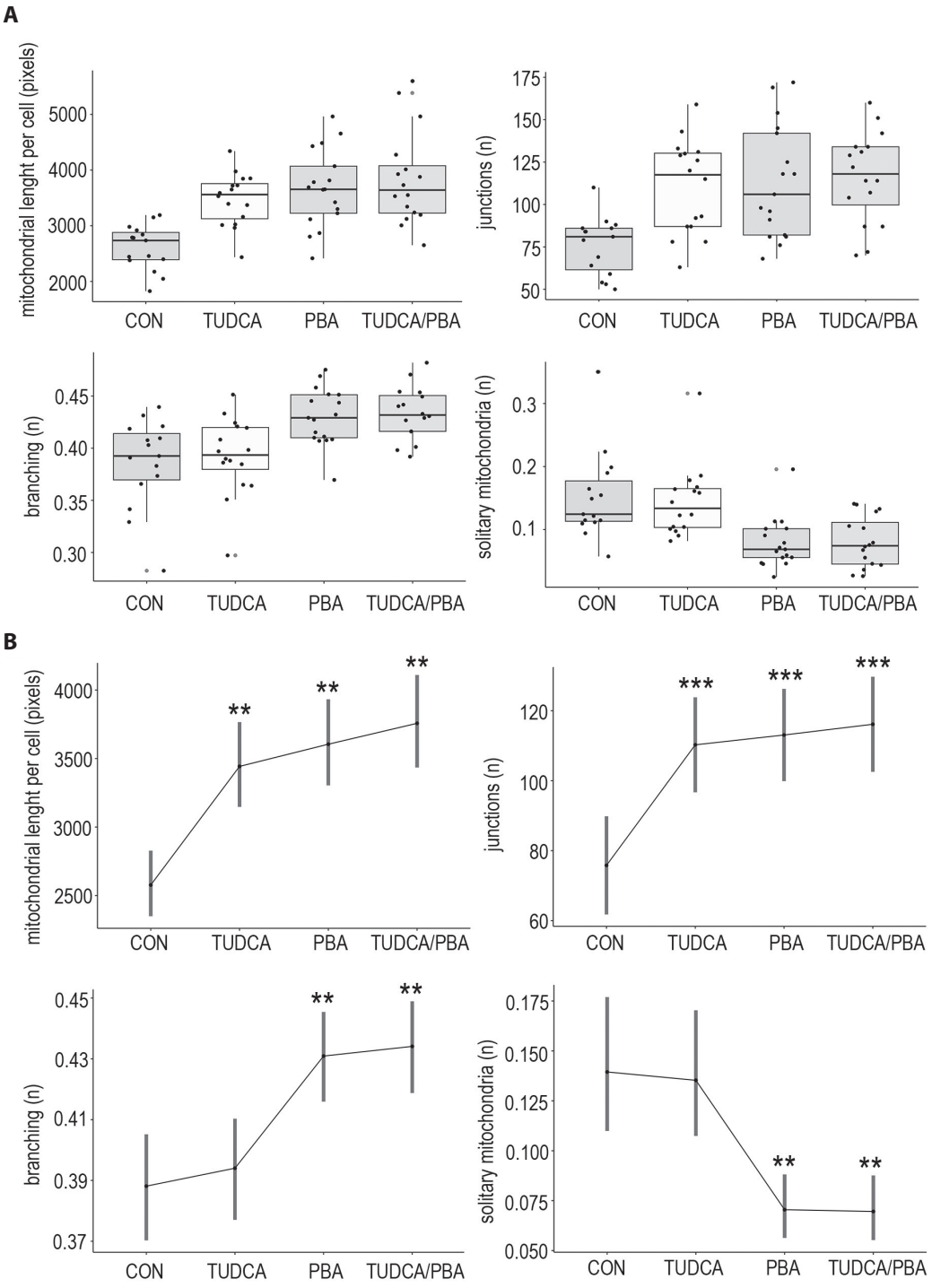

Figure 3. Impact of TUDCA and PBA on mitochondrial network parameters. **A.** Graphical presentation of the distribution of mitochondrial network parameters across experimental groups. Boxplots visualizing mitochondrial network parameters across experimental groups. The box represents data between the lower and upper quartiles, with a line marking the median. Whiskers are determined by the lower quartile minus 1.5×interquartile range and the upper quartile plus 1.5×interquartile range. **B.** Back-transformed emmeans for overall mitochondrial length, branching, junctions and solitary rod-like mitochondria in experimental groups with 95% confidence interval. The final binary images obtained from raw images of the mitochondrial network were analysed as described in Material and Methods. ** $p < 0.01$, *** $p < 0.001$ (Pairwise comparisons, with Tukey adjustment of p-values, were performed to further evaluate differences between mitochondrial network parameters of treated cells compared to the control non-treated cells).

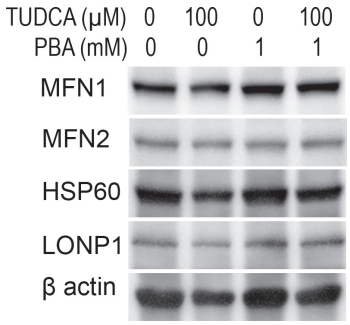

Figure 4. Impact of TUDCA and PBA on the expression of mitochondrial proteins. Total cell extracts were prepared from SH-SY5Y cells after treatment with TUDCA, PBA and combination of TUDCA with PBA for 16 h. The effect of the treatments on the levels of MFN1, MFN2, HSP60 and LONP1 was evaluated by Western blot analysis of total cell extracts as described in Materials and Methods. β-actin served as the loading control. The representative images of 4 independent experiments are cropped from different parts of the same blot.

represents the main cellular response to ER stress, as well as the cytoprotective mechanism to cope with stress-inducing conditions and to restore ER homeostasis and functions (Almanza et al. 2019). HRD1 is an E3 ligase involved in the process of ER-associated degradation (ERAD) (Kikkert et al. 2004) that includes retro-translocation of aberrant proteins from ER to the cytosol through the membrane spanning retro-translocon (Hampton and Sommer 2012), polyubiquitinylation of aberrant proteins by means of HRD1 and final degradation of aberrant proteins by the 26S proteasome (Preston and Brodsky 2017). The interaction of HRD1 with SEL1L is a prerequisite for the formation of a functional HRD1-ERAD complex (Lin et al. 2024); therefore, we have also analysed the expression of SEL1L.

In agreement with our previous study (Dibdiakova et al. 2019), treatment of the cells for 24 h with tunicamycin at a concentration of 2 μM (Fig. 5) was associated with significant increase of HRD1 expression (225% of control, $p < 0.05$).

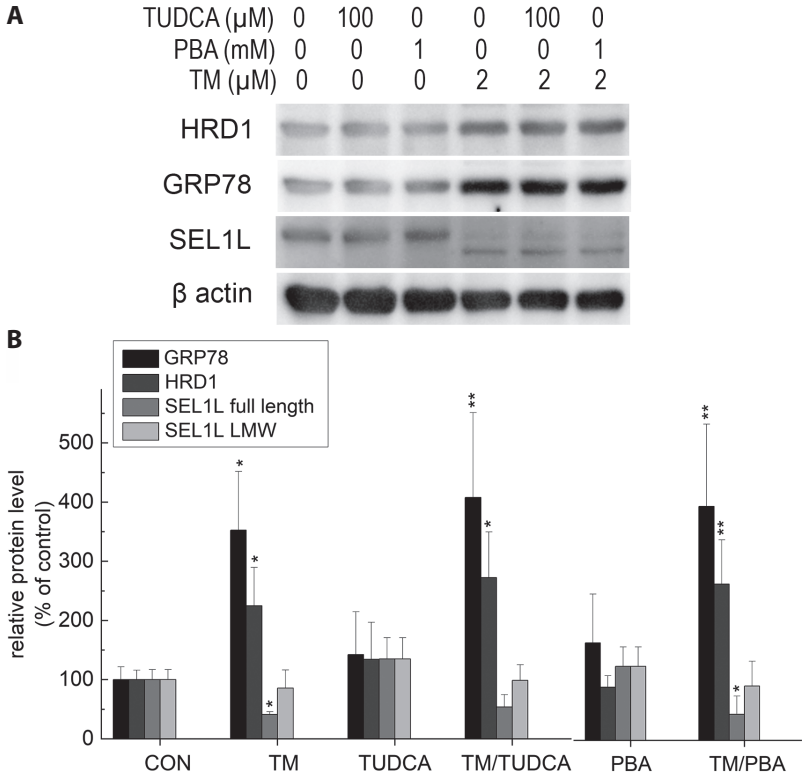

Figure 5. Impact of TUDCA or PBA on tunicamycin-induced expression of HRD1, GRP78 and SEL1L. **A.** The representative images of 4 independent experiments that were cropped from different parts of the same blot. **B.** Quantitative evaluation of the impact of TUDCA or PBA on tunicamycin-induced expression of HRD1, GRP78 and SEL1L. Total cell extracts were prepared from SH-SY5Y cells that were first pre-treated with TUDCA or PBA for 16 h that was followed by treatment of the cells with tunicamycin at a concentration of 2 μM for 24 h in the presence of either TUDCA or PBA. The effect of the treatments on the levels of HRD1, GRP78 and SEL1L was evaluated by Western blot analysis of total cell extracts as described in Materials and Methods. HRD1, GRP78 and SEL1L levels were normalized to β-actin levels and are expressed as relative to non-treated controls. Data are presented as means ± SD (4 independent experiments *per* each treatment). * $p < 0.05$, ** $p < 0.01$ (two-way ANOVA, followed by Tukey's test to determine differences between the levels of analysed proteins in control non-treated cells and treated cells). LMW, low molecular weight.

The expression of GRP78 was also significantly increased in the cells treated with tunicamycin (352.6% of control, $p < 0.01$). With respect to SEL1L, we have observed the expression of protein with significantly lower molecular weight after the treatment of the cells for 24 h with tunicamycin at a concentration of 2 μM (Fig. 5). Since SEL1L contains five putative N-glycosylation sites (Jeong et al. 2016) production of lower molecular weight protein could be explained by inhibition of N-glycosylation of SEL1L polypeptide *via* tunicamycin that is a potent inhibitor of N-glycosylation located in ER, thereby inducing ER stress (Almanza et al. 2019). We have observed that intensity of the band representing full length protein was significantly decreased (41.4% of control, $p < 0.05$) after the treatment of the cells for 24 h with tunicamycin at a concentration of 2 μM (Fig. 5). Intensity of the band representing low molecular weight protein was not significantly altered after the treatment of the cells for 24 h with tunicamycin at a concentration of 2 μM (Fig. 5B). Neither TUDCA nor PBA have significantly changed the level of expression of GRP78, HRD1 and SEL1L (Fig. 5B). In cells pre-treated with TUDCA (Fig. 5B), treatment with tunicamycin increased significantly expression of both GRP78 (389.5% of control, $p < 0.01$) and HRD1 (264% of control, $p < 0.05$) and decreased expression of full length SEL1L (53.9% of control, $p = 0.0557$). In cells pre-treated with PBA (Fig. 5B), treatment with tunicamycin increased significantly expression of both GRP78 (408% of control, $p < 0.01$) and HRD1 (272.5% of control, $p < 0.01$) and decreased significantly expression of full length SEL1L (45.5% of control, $p < 0.05$). Thus, pre-treatment of the cells with either TUDCA or PBA did not significantly affect changes of the expression of HRD1, GRP78 and SEL1L induced by tunicamycin.

Discussion

In the present study, we have shown that both TUDCA and PBA, as well as combination of TUDCA with PBA, have a significant impact on mitochondrial respiration. Although both substances are considered to work as chemical chaperones, they affect mitochondrial respiration in a specific way. While TUDCA decreases ROUTINE respiration, maximal respiration, succinate-driven maximal respiration, ATP-coupled respiration and leak respiration; PBA increases SRC. Interestingly, pre-treatment of the cell with combination of TUDCA with PBA resulted in an increase of ROUTINE respiration, maximal respiration, succinate driven maximal respiration, ATP-coupled respiration and SRC. Both TUDCA and PBA, as well as combination of TUDCA with PBA, exhibit an impact on elongation of mitochondria. The intracellular ATP concentration did not change significantly after incubation of the cells with both TUDCA and PBA as well as combination of TUDCA with PBA. Both TUDCA and PBA, as well as combination of TUDCA with PBA, did not affect the expression of the investigated mitochondrial proteins. Finally, our results do not indicate the ability of TUDCA and PBA to alleviate ER stress.

Although TUDCA deceases all parameters of mitochondrial respiration determined in this study, we did not observe significant changes of intracellular ATP concentration after incubation of the cells with TUDCA. Unaltered ATP level was also documented after incubation of SH-SY5Y cells for 12 h with 0.1 mM TUDCA (Fonseca et al. 2017; Rosa et al. 2017) while ATP was significantly increased in primary murine cortical neurons incubated for 12 h with 0.1 mM TUDCA (Rosa et al. 2017). In animal models of PD using mitochondrial toxins, the neuroprotective effects of TUDCA were among other mechanisms attributed to the reduction of mitochondrial dysfunction induced oxidative stress (Castro-Caldas et al. 2012; Moreira et al. 2017; Cuevas et al. 2022). In cellular model of Huntington's disease, TUDCA prevented decrease of mitochondrial transmembrane potential induced by 3-nitropropionic acid (Rodrigues et al. 2000). Our experiments revealed possible positive impact of TUDCA on the inner mitochondrial membrane that was associated with a significant decrease of leak respiration. TUDCA mediated stabilisation of mitochondrial membrane was also documented earlier (Fonseca et al. 2017), but the involvement of such mechanism in neuroprotective effects of TUDCA is unclear.

While PBA has no significant impact on ROUTINE, maximal and ATP-coupled respiration, treatment of the cells with PBA results in a significant increase of SRC. Increased SRC together with increased basal and maximal respiration was documented in 3T3-L1 adipocytes treated with 1 mM PBA for 2 days (Tanis et al. 2015). In turn, higher concentrations of PBA had an inhibitory impact on mitochondrial functions (Tanis et al. 2015). Although, SRC is a well-recognised phenomenon (Nicholls 2009; Marchetti et al. 2020), the molecular components of SRC and the factors that determine SRC are not well described. The potential of SRC to increase ATP supply and, therefore, to avoid an 'ATP crisis' during the periods of increased energy demands (e.g., an increased workload or cellular activity that is typical for firing neurons) is generally accepted. As documented previously, reduced SRC correlates with increased sensitivity of cells to cell death inducing agents (Yadava and Nicholls 2007), while increased SRC correlates well with cell resistance and enhanced cell survival (Nickens et al. 2013; Pfleger et al. 2015).

Although basal and maximal respiration was unaltered in C12 cells treated with 0.5 mM PBA for 24 h, PBA increased mitochondrial biogenic signalling, function and content (Rivera et al. 2024). On the contrary, 10 mM PBA reduced mitochondrial function and content. The expression levels

of mitochondrial biogenesis-related proteins and mitochondrial antioxidant responses were also significantly increased by TUDCA in subventricular zone-derived neural stem cells (Soares et al. 2018). Results of our Western blot analysis documented the unaltered expression of mitochondrial proteins, including HSP60, which can be considered as a marker of intracellular mitochondria content; do not support the possibility of enhanced mitochondrial biogenesis caused by treatment of the SH-SY5Y cells with either TUDCA or PBA. Combination of TUDCA with PBA has even more significant impact on mitochondrial respiration but it did not affect expression of mitochondrial proteins as well.

Our results showing an impact of TUDCA and PBA as well as combination of TUDCA with PBA on mitochondrial network are indicating their possible impact on mitochondrial morphology supporting mitochondrial fusion and preventing mitochondrial fission. With respect to combination of TUDCA with PBA, the results are in agreement with a current view that fused mitochondria, prevalent in healthy metabolically active cells, exhibit a higher ATP production, while fragmented mitochondria, which are encountered in quiescent and metabolically inactive cells, exhibit reduced respiration and are associated with different pathological conditions (Chen et al. 2023). Previous study indirectly indicated impact of TUDCA on mitochondrial network associated with elongation of mitochondria (Rosa et al. 2017). Treatment of mouse embryonic fibroblasts with PBA, which results in peroxisome proliferation, resulted in mitochondrial elongation (Tanaka et al. 2019). On contrary, both PBA (50 μM) and TUDCA (100 μM) showed little effects on mitochondrial morphology mitochondrial reactive oxygen species in pulmonary artery smooth muscle cell (Zhuan et al. 2020). In our recent study, we have documented more developed mitochondrial network that can be attributed to mitochondrial fusion in differentiated SH-SY5Y cells compared to non-differentiated SH-SY5Y cells (Evinova et al. 2024). Changes in the mitochondrial network were accompanied with significantly increased mitochondrial respiration in differentiated cells. In turn, the mitochondrial network was changed toward more fragmented mitochondria after treatment of the cells with rotenone (Evinova et al. 2024). Similar shift of the mitochondrial network towards mitochondrial fragmentation was observed in fibroblasts of patients with mitochondrial disorders (Bakare et al. 2021) or in fibroblasts of patients with Parkinson's disease (Kritskaya et al. 2024). We did not observe changes in expression of main proteins involved in regulation of mitochondrial fusions, but other proteins and mechanism that can be considered, e.g. post-translation modifications of fusion proteins, cannot be excluded (Giacomello et al. 2020; Chen et al. 2023). In addition, elongation of mitochondria could be a result of adaptive remodeling of mitochondrial membrane phosphatidic acid (Perea et al. 2023).

Both TUDCA and PBA are considered to work as chemical chaperones with a positive impact on ER stress (Almanza et al. 2019; Jeon et al. 2022). At the molecular level, ER stress is characterised by upregulation of specific proteins like GRP78, ER resident chaperone (Almanza et al. 2019), and HRD1, ER resident E3 ligase (Preston and Brodsky 2017). Overexpression of GRP78 increases ER chaperone capacity while overexpression of HRD1 increases capacity of removal of aberrant proteins from ER (Almanza et al. 2019). Interaction of HRD1 with SEL1L is a prerequisite for the formation of a functional HRD1-ERAD complex. ER stress is also associated with mitochondrial dysfunction as documented in several previous studies (Carreras-Sureda et al. 2019; Evinova et al. 2022). As one of the possible explanations of ER stress-induced mitochondrial dysfunction, it was shown that HRD1 down-regulates level of PGC1β resulting in decreased mitochondrial biogenesis (Fujita et al. 2015). In addition, acute ER stress is associated with elongation of mitochondria as a result of adaptive remodeling of mitochondrial membrane phosphatidic acid (Perea et al. 2023). In agreement with our previous study (Dibdiakova et al. 2019), tunicamycin induced increased expression of HRD1. The expression of GRP78 was also increased in response to tunicamycin. In cell treated with tunicamycin, we have also observed decreased expression of full length SEL1L protein and appearance of low molecular weight SEL1L protein that could be attributed to the inhibition of N-glycosylation with tunicamycin. Neither TUDCA nor PBA have changed the level of expression of GRP78, HRD1 and SEL1L. In addition, both TUDCA and PBA did not affect the tunicamycin-induced changes in the expression of GRP78, HRD1 and SEL1L. We suppose that neither TUDCA nor PBA affect ER stress response at the level of the expression of GRP78, HRD1 and SEL1L. Our results do not indicate the ability of either TUDCA or PBA to alleviate ER stress.

In conclusion, we have shown that both TUDCA and PBA as well as combination of TUDCA with PBA have important impact on mitochondrial functions and morphology. The impact of PBA and combination of TUDCA with PBA on mitochondrial functions might be associated with possible neuroprotective effects of PBA and combination of TUDCA with PBA. Although TUDCA exhibited positive effect on inner mitochondrial membrane, the possible neuroprotective effect of TUDCA might involve another mechanism distinct from the TUDCA-mediated modification of mitochondrial functions.

Conflict of interest. The authors declare that there are no conflicts of interest.

Acknowledgements. This work was supported by grant VEGA 1/0183/23 from Scientific Grant Agency of the Ministry of Education, Science, Research and Sport of the Slovak Republic.

References

Almanza A, Carlesso A, Chintha C, Creedican S, Doultsinos D, Leuzzi B, Luís A, McCarthy N, Montibeller L, More S, et al. (2019): Endoplasmic reticulum stress signalling – from basic mechanisms to clinical applications. FEBS J. **286,** 241-278 https://doi.org/10.1111/febs.14608

Albanese A, Ludolph AC, McDermott CJ, Corcia P, Van Damme P, Van den Berg LH, Hardiman O, Rinaldi G, Vanacore N, Dickie B, TUDCA-ALS Study Group (2022): Tauroursodeoxycholic acid in patients with amyotrophic lateral sclerosis: The TUDCA-ALS trial protocol. Front. Neurol. **13,** 1009113 https://doi.org/10.3389/fneur.2022.1009113

Alqallaf A, Cates DW, Render KP, Patel KA (2024): Sodium phenylbutyrate and taurursodiol: A new therapeutic option for the treatment of amyotrophic lateral sclerosis. Ann. Pharmacother. **58,** 165-173 https://doi.org/10.1177/10600280231172802

Anwer MS, Stieger B (2014): Sodium-dependent bile salt transporters of the SLC10A transporter family: more than solute transporters. Pflugers Arch. **466,** 77-89 https://doi.org/10.1007/s00424-013-1367-0

Bakare AB, Daniel J, Stabach J, Rojas A, Bell A, Henry B, Iyer S (2021): Quantifying mitochondrial dynamics in patient fibroblasts with multiple developmental defects and mitochondrial disorders. Int. J. Mol. Sci. **22,** 6263 https://doi.org/10.3390/ijms22126263

Cappellacci L, Perinelli DR, Maggi F, Grifantini M, Petrelli R (2020): Recent progress in histone deacetylase inhibitors as anticancer agents. Curr. Med. Chem. **27,** 2449-2493 https://doi.org/10.2174/0929867325666181016163110

Carreras-Sureda A, Jaña F, Urra H, Durand S, Mortenson D. E, Sagredo A, Bustos G, Hazari Y, Ramos-Fernández E, Sassano ML, et al. (2019): Non-canonical function of IRE1α determines mitochondria-associated endoplasmic reticulum composition to control calcium transfer and bioenergetics. Nat. Cell Biol. **21,** 755-767 https://doi.org/10.1038/s41556-019-0329-y

Castro-Caldas M, Carvalho A. N, Rodrigues E, Henderson CJ, Wolf CR, Rodrigues CM, Gama MJ (2012): Tauroursodeoxycholic acid prevents MPTP-induced dopaminergic cell death in a mouse model of Parkinson's disease. Mol. Neurobiol. **46,** 475-486 https://doi.org/10.1007/s12035-012-8295-4

Chen W, Zhao H, Li Y (2023): Mitochondrial dynamics in health and disease: mechanisms and potential targets. Signal. Transduct. Target Ther. **8,** 333 https://doi.org/10.1038/s41392-023-01547-9

Cuevas E, Burks S, Raymick J, Robinson B, Gómez-Crisóstomo NP, Escudero-Lourdes C, Lopez AGG, Chigurupati S, Hanig J, Ferguson SA, Sarkar S (2022): Tauroursodeoxycholic acid (TUDCA) is neuroprotective in a chronic mouse model of Parkinson's disease. Nutr. Neurosci. **25,** 1374-1391 https://doi.org/10.1080/1028415X.2020.1859729

Dibdiakova K, Saksonova S, Pilchova I, Klacanova K, Tatarkova Z, Racay P (2019): Both thapsigargin- and tunicamycin-induced endoplasmic reticulum stress increases expression of Hrd1 in IRE1-dependent fashion. Neurol. Res. **41,** 177-188 https://doi.org/10.1080/01616412.2018.1547856

Duarte-Silva S, Da Silva JD, Monteiro-Fernandes D, Costa MD, Neves-Carvalho A, Raposo M, Soares-Cunha C, Correia JS, Nogueira-Goncalves G, Fernandes HS, et al. (2024): Glucocorticoid receptor-dependent therapeutic efficacy of tauroursodeoxycholic acid in preclinical models of spinocerebellar ataxia type 3. J. Clin. Invest. **134,** e162246 https://doi.org/10.1172/JCI162246

Evinova A, Cizmarova B, Hatokova Z, Racay P (2020): High-resolution respirometry in assessment of mitochondrial function in neuroblastoma SH-SY5Y intact cells. J. Membr. Biol. **253,** 129-136 https://doi.org/10.1007/s00232-020-00107-4

Evinova A, Hatokova Z, Tatarkova Z, Brodnanova M, Dibdiakova K, Racay P (2022): Endoplasmic reticulum stress induces mitochondrial dysfunction but not mitochondrial unfolded protein response in SH-SY5Y cells. Mol. Cell. Biochem. **477,** 965-975 https://doi.org/10.1007/s11010-021-04344-6

Evinova A, Baranovicova E, Hajduchova D, Dibdiakova K, Baranova I, Racay P, Strnadel J, Pecova R, Halasova E, Pokusa M (2024): The impact of ATP-sensitive potassium channel modulation on mitochondria in a Parkinson's disease model using SH-SY5Y cells depends on their differentiation state. J. Bioenerg. Biomembr. **56,** 347-360 https://doi.org/10.1007/s10863-024-10018-x

Fiorese CJ, Schulz AM, Lin YF, Rosin N, Pellegrino MW, Haynes CM. (2016): The transcription factor ATF5 mediates a mammalian mitochondrial UPR. Curr. Biol. **26,** 2037-2043 https://doi.org/10.1016/j.cub.2016.06.002

Fonseca I, Gordino G, Moreira S, Nunes MJ, Azevedo C, Gama MJ, Rodrigues E, Rodrigues CMP, Castro-Caldas M (2017): Tauroursodeoxycholic acid protects against mitochondrial dysfunction and cell death via mitophagy in human neuroblastoma cells. Mol. Neurobiol. **54,** 6107-6119 https://doi.org/10.1007/s12035-016-0145-3

Fox J, Weisberg S, Price B (2023): An R Companion to Applied Regression (4th Ed.), SAGE Publications, Inc.

Fujita H, Yagishita N, Aratani S, Saito-Fujita T, Morota S, Yamano Y, Hansson MJ, Inazu M, Kokuba H, Sudo K, et al. (2015) The E3 ligase synoviolin controls body weight and mitochondrial biogenesis through negative regulation of PGC-1β. EMBO J. **34,** 1042-1055 https://doi.org/10.15252/embj.201489897

Giacomello M, Pyakurel A, Glytsou C, Scorrano L (2020): The cell biology of mitochondrial membrane dynamics. Nat. Rev. Mol. Cell. Biol. **21,** 204-224 https://doi.org/10.1038/s41580-020-0210-7

Hampton RY, Sommer T (2012) Finding the will and the way of ERAD substrate retrotranslocation. Curr. Opin. Cell Biol. **24,** 460-466 https://doi.org/10.1016/j.ceb.2012.05.010

He B, Moreau R (2019): Lipid-regulating properties of butyric acid and 4-phenylbutyric acid: Molecular mechanisms and therapeutic applications. Pharmacol. Res. **144,** 116-131 https://doi.org/10.1016/j.phrs.2019.04.002

Jeon JH, Im S, Kim HS, Lee D, Jeong K, Ku JM, Nam TG (2022): Chemical chaperones to inhibit endoplasmic reticulum

stress: Implications in diseases. Drug. Des. Devel. Ther. **16,** 4385-4397
https://doi.org/10.2147/DDDT.S393816

Jeong H, Sim HJ, Song EK, Lee H, Ha SC, Jun Y, Park TJ, Lee C (2016): Crystal structure of SEL1L: Insight into the roles of SLR motifs in ERAD pathway. Sci. Rep. **6,** 20261
https://doi.org/10.1038/srep20261

Jurica J, Dovrtelová G, Noskova K, Zendulka O (2016): Bile acids, nuclear receptors and cytochrome P450. Physiol. Res. **65,** S427-S440
https://doi.org/10.33549/physiolres.933512

Ketabforoush A, Faghihi F, Azedi F, Ariaei A, Habibi MA, Khalili M, Ashtiani BH, Joghataei MT, Arnold WD (2024): Sodium phenylbutyrate and tauroursodeoxycholic acid: A story of hope turned to disappointment in amyotrophic lateral sclerosis treatment. Clin. Drug Investig. **44,** 495-512
https://doi.org/10.1007/s40261-024-01371-1

Khalaf K, Tornese P, Cocco A, Albanese A (2022): Tauroursodeoxycholic acid: a potential therapeutic tool in neurodegenerative diseases. Transl. Neurodegener. **11,** 33
https://doi.org/10.1186/s40035-022-00307-z

Kikkert M, Doolman R, Dai M, Avner R, Hassink G, van Voorden S, Thanedar S, Roitelman J, Chau V, Wiertz E (2004): Human HRD1 is an E3 ubiquitin ligase involved in degradation of proteins from the endoplasmic reticulum. J. Biol. Chem. **279,** 3525-3534
https://doi.org/10.1074/jbc.M307453200

Klacanova K, Pilchova I, Klikova K, Racay P (2016): Short chemical ischemia triggers phosphorylation of eIF2α and death of SH-SY5Y cells but not proteasome stress and heat shock protein response in both SH-SY5Y and T98G cells. J. Mol. Neurosci. **58,** 497-506
https://doi.org/10.1007/s12031-015-0685-4

Kolb PS, Ayaub EA, Zhou W, Yum V, Dickhout JG, Ask K (2015): The therapeutic effects of 4-phenylbutyric acid in maintaining proteostasis. Int. J. Biochem. Cell Biol. **61,** 45-52
https://doi.org/10.1016/j.biocel.2015.01.015

Kritskaya KA, Fedotova EI, Berezhnov AV (2024): Impaired mitochondrial network morphology and reactive oxygen species production in fibroblasts from Parkinson's disease patients. Biomedicines **12,** 282
https://doi.org/10.3390/biomedicines12020282

Kusaczuk M (2019): Tauroursodeoxycholate-bile acid with chaperoning Activity: Molecular and cellular effects and therapeutic perspectives. Cells **8,** 1471
https://doi.org/10.3390/cells8121471

Kusaczuk M, Bartoszewicz M, Cechowska-Pasko M (2015): Phenylbutyric acid: simple structure - multiple effects. Curr. Pharm. Des. **21,** 2147-2166
https://doi.org/10.2174/1381612821666150105160059

Lin LL, Wang HH, Pederson B, Wei X, Torres M, Lu Y, Li ZJ, Liu X, Mao H, Wang H, et al. (2024): SEL1L-HRD1 interaction is required to form a functional HRD1 ERAD complex. Nat. Commun. **17,** 1440
https://doi.org/10.1101/2023.04.13.536796

Lombardo FL, Spila Alegiani S, Mayer F, Cipriani M, Lo Giudice M, Ludolph AC, McDermott CJ, Corcia P, Van Damme P, Van den Berg LH, et al. (2023): A randomized double-blind clinical trial on safety and efficacy of tauroursodeoxycholic acid (TUDCA) as add-on treatment in patients affected by amyotrophic lateral sclerosis (ALS): the statistical analysis plan of TUDCA-ALS trial. Trials **24,** 792
https://doi.org/10.1186/s13063-023-07638-w

Marchetti P, Fovez Q, Germain N, Khamari R, Kluza J (2020): Mitochondrial spare respiratory capacity: Mechanisms, regulation, and significance in non-transformed and cancer cells. FASEB J. **34,** 13106-13124
https://doi.org/10.1096/fj.202000767R

Moreira S, Fonseca I, Nunes MJ, Rosa A, Lemos L, Rodrigues E, Carvalho AN, Outeiro TF, Rodrigues CMP, Gama MJ, Castro-Caldas M (2017): Nrf2 activation by tauroursodeoxycholic acid in experimental models of Parkinson's disease. Exp. Neurol. **295,** 77-87
https://doi.org/10.1016/j.expneurol.2017.05.009

Nicholls DG (2009): Spare respiratory capacity, oxidative stress and excitotoxicity. Biochem. Soc. Trans. **37,** 1385-1388
https://doi.org/10.1042/BST0371385

Nickens KP, Wikstrom JD, Shirihai OS, Patierno SR, Ceryak S (2013): A bioenergetic profile of nontransformed fibroblasts uncovers a link between death-resistance and enhanced spare respiratory capacity. Mitochondrion **13,** 662-667
https://doi.org/10.1016/j.mito.2013.09.005

Paganoni S, Quintana M, Sherman AV, Vestrucci M, Wu Y, Timmons J, Cudkowicz M, Pooled Resource Open-Access ALS Clinical Trials Consortium (2023): Analysis of sodium phenylbutyrate and taurursodiol survival effect in ALS using external controls. Ann. Clin. Transl. Neurol. **10,** 2297-2304
https://doi.org/10.1002/acn3.51915

Perea V, Cole C, Lebeau J, Dolina V, Baron KR, Madhavan A, Kelly JW, Grotjahn DA, Wiseman RL (2023): PERK signaling promotes mitochondrial elongation by remodeling membrane phosphatidic acid. EMBO J. **42,** e113908
https://doi.org/10.15252/embj.2023113908

Pesta D, Gnaiger E (2012): High-resolution respirometry: OXPHOS protocols for human cells and permeabilized fibers from small biopsies of human muscle. Methods Mol. Biol. **810,** 25-58
https://doi.org/10.1007/978-1-61779-382-0_3

Pfleger J, He M, Abdellatif M (2015): Mitochondrial complex II is a source of the reserve respiratory capacity that is regulated by metabolic sensors and promotes cell survival. Cell Death Dis. **6,** e1835
https://doi.org/10.1038/cddis.2015.202

Preston GM, Brodsky JL (2017) The evolving role of ubiquitin modification in endoplasmic reticulum-associated degradation. Biochem. J. **474,** 445-469
https://doi.org/10.1042/BCJ20160582

Rivera CN, Smith CE, Draper LV, Watne RM, Wommack AJ, Vaughan RA (2024): Physiological 4-phenylbutyrate promotes mitochondrial biogenesis and metabolism in C2C12 myotubes. Biochimie **219,** 155-164
https://doi.org/10.1016/j.biochi.2023.11.009

Rodrigues CM, Stieers CL, Keene CD, Ma X, Kren BT, Low WC, Steer CJ (2000): Tauroursodeoxycholic acid partially prevents apoptosis induced by 3-nitropropionic acid: evidence for a mitochondrial pathway independent of the permeability transition. J. Neurochem. **75,** 2368-2379

https://doi.org/10.1046/j.1471-4159.2000.0752368.x
Rosa AI, Fonseca I, Nunes MJ, Moreira S, Rodrigues E, Carvalho AN, Rodrigues CMP, Gama MJ, Castro-Caldas M (2017): Novel insights into the antioxidant role of tauroursodeoxycholic acid in experimental models of Parkinson's disease. Biochim. Biophys. Acta Mol. Basis Dis. **1863,** 2171-2181 https://doi.org/10.1016/j.bbadis.2017.06.004
Soares R, Ribeiro FF, Xapelli S, Genebra T, Ribeiro MF, Sebastião AM, Rodrigues CMP, Solá S (2018): Tauroursodeoxycholic acid enhances mitochondrial biogenesis, neural stem cell pool, and early neurogenesis in adult rats. Mol. Neurobiol. **55,** 3725-3738 https://doi.org/10.1007/s12035-017-0592-5
Sun Y, Li X, Bedlack R (2023): An evaluation of the combination of sodium phenylbutyrate and taurursodiol for the treatment of amyotrophic lateral sclerosis. Expert Rev. Neurother. **23,** 1-7 https://doi.org/10.1080/14737175.2023.2174018
Tanaka H, Okazaki T, Aoyama S, Yokota M, Koike M, Okada Y, Fujiki Y, Gotoh Y (2019): Peroxisomes control mitochondrial dynamics and the mitochondrion-dependent apoptosis pathway. J. Cell Sci. **132,** jcs224766 https://doi.org/10.1242/jcs.224766
Tanis RM, Piroli GG, Day SD, Frizzell N (2015): The effect of glucose concentration and sodium phenylbutyrate treatment on mitochondrial bioenergetics and ER stress in 3T3-L1 adipocytes. Biochim. Biophys. Acta **1853,** 213-221 https://doi.org/10.1016/j.bbamcr.2014.10.012
Wright G, Noiret L, Olde Damink SW, Jalan R (2011): Interorgan ammonia metabolism in liver failure: the basis of current and future therapies. Liver Int. **31,** 163-175 https://doi.org/10.1111/j.1478-3231.2010.02302.x
Xing C, Huang X, Wang D, Yu D, Hou S, Cui H, Song L (2023): Roles of bile acids signaling in neuromodulation under physiological and pathological conditions. Cell Biosci. **13,** 106 https://doi.org/10.1186/s13578-023-01053-z
Yadava N, Nicholls DG (2007): Spare respiratory capacity rather than oxidative stress regulates glutamate excitotoxicity after partial respiratory inhibition of mitochondrial complex I with rotenone. J. Neurosci. **27,** 7310-7317 https://doi.org/10.1523/JNEUROSCI.0212-07.2007
Zangerolamo L, Vettorazzi JF, Rosa LRO, Carneiro EM, Barbosa HCL (2021): The bile acid TUDCA and neurodegenerative disorders: An overview. Life Sci. **272,** 119252 https://doi.org/10.1016/j.lfs.2021.119252
Zhuan B, Wang X, Wang MD, Li ZC, Yuan Q, Xie J, Yang Z (2020): Hypoxia induces pulmonary artery smooth muscle dysfunction through mitochondrial fragmentation-mediated endoplasmic reticulum stress. Aging **12,** 23684-23697 https://doi.org/10.18632/aging.103892

Received: December 9, 2024
Final version accepted: April 29, 2025